0090-9556/10/3804-617–625$20.00
DRUG METABOLISM AND DISPOSITION
Vol. 38, No. 4
31047/3569496
DMD 38:617–625, 2010
Printed in U.S.A.

Phase II Metabolism of Hesperetin by Individual UDP-Glucuronosyltransferases and Sulfotransferases and Rat and Human Tissue Samples

Walter Brand, Marelle G. Boersma, Hanneke Bik, Elisabeth F. Hoek-van den Hil, Jacques Vervoort, Denis Barron, Walter Meinl, Hansruedi Glatt, Gary Williamson, Peter J. van Bladeren, and Ivonne M. C. M. Rietjens

Division of Toxicology, Wageningen University, Wageningen, The Netherlands (W.B., M.G.B., H.B., E.F.H.v.d.H., P.J.v.B., I.M.C.M.R.); Nestlé Research Center, Nestec Ltd., Lausanne, Switzerland (W.B., D.B., G.W., P.J.v.B.); Biqualys, Wageningen, The Netherlands (J.V.); Department of Nutritional Toxicology, German Institute of Human Nutrition, Potsdam-Rehbrücke, Nuthetal, Germany (W.M., H.G.); and School of Food Science and Nutrition, University of Leeds, Leeds, United Kingdom (G.W.)

Received November 5, 2009; accepted January 7, 2010

ABSTRACT:

Phase II metabolism by UDP-glucuronosyltransferases (UGTs) and sulfotransferases (SULTs) is the predominant metabolic pathway during the first-pass metabolism of hesperetin (4′-methoxy-3′,5,7-trihydroxyflavanone). In the present study, we have determined the kinetics for glucuronidation and sulfonation of hesperetin by 12 individual UGT and 12 individual SULT enzymes as well as by human or rat small intestinal, colonic, and hepatic microsomal and cytosolic fractions. Results demonstrate that hesperetin is conjugated at positions 7 and 3′ and that major enzyme-specific differences in kinetics and regioselectivity for the UGT and SULT catalyzed conjugations exist. UGT1A9, UGT1A1, UGT1A7, UGT1A8, and UGT1A3 are the major enzymes catalyzing hesperetin glucuronidation, the latter only producing 7-*O*-glucuronide, whereas UGT1A7 produced mainly 3′-*O*-glucuronide. Furthermore, UGT1A6 and UGT2B4 only produce hesperetin 7-*O*-glucuronide, whereas UGT1A1, UGT1A8, UGT1A9, UGT1A10, UGT2B7, and UGT2B15 conjugate both positions. SULT1A2 and SULT1A1 catalyze preferably and most efficiently the formation of hesperetin 3′-*O*-sulfate, and SULT1C4 catalyzes preferably and most efficiently the formation of hesperetin 7-*O*-sulfate. Based on expression levels SULT1A3 and SULT1B1 also will probably play a role in the sulfo-conjugation of hesperetin in vivo. The results help to explain discrepancies in metabolite patterns determined in tissues or systems with different expression of UGTs and SULTs, e.g., hepatic and intestinal fractions or Caco-2 cells. The incubations with rat and human tissue samples support an important role for intestinal cells during first-pass metabolism in the formation of hesperetin 3′-*O*-glucuronide and 7-*O*-glucuronide, which appear to be the major hesperetin metabolites found in vivo.

The flavanone hesperetin (4′-methoxy-3′,5,7-trihydroxyflavanone) (Fig. 1) is the aglycone of hesperidin (hesperetin 7-*O*-rutinoside), which is the major flavonoid present in sweet oranges (*Citrus sinensis*) and orange juice and also occurs in other citrus fruits and some herbs (Tomás-Barberán and Clifford, 2000). Hesperidin and hesperetin have been reported to provide beneficial effects on health, including reduced risk of osteoporosis (Horcajada et al., 2008).

Upon ingestion, hesperidin has to be hydrolyzed into hesperetin aglycone by colonic microbiota before its absorption (Németh et al., 2003). Enzymatic conversion of hesperidin before consumption to the monosaccharide hesperetin-7-*O*-glucoside has been demonstrated to result in absorption in the small intestine after deglucosylation by phloridzin hydrolase and/or facilitated transport into the intestinal cells by a sugar transporter such as sodium-glucose cotransporter 1 followed by intracellular deglucosylation (Nielsen et al., 2006). In the intestinal cells or during further first-pass metabolism, hesperetin aglycone is metabolized by UDP-glucuronosyltransferases (UGTs) and sulfotransferases (SULTs) into, respectively, glucuronidated and sulfonated metabolites, which have been detected in human and rat plasma (Manach et al., 2003; Matsumoto et al., 2004; Mullen et al., 2008; Brett et al., 2009). The intestinal barrier is believed to play a dominant role in phase II conjugation during the first-pass metabolism of hesperetin (Silberberg et al., 2006) and in its limited bioavailability because of efflux of the metabolites back to the intestinal lumen by ABC transport proteins (Liu and Hu, 2007; Brand et al., 2008).

UGTs form a gene superfamily and currently a total of 22 different UGT proteins have been detected in human tissues, belonging to either the UGT1A (UGT1A1, UGT1A3, UGT1A4, UGT1A5, UGT1A6, UGT1A7, UGT1A8, UGT1A9, and UGT1A10), the

This study was supported by the Nestlé Research Center, Nestec Ltd. (Lausanne, Switzerland).

Article, publication date, and citation information can be found at http://dmd.aspetjournals.org.

doi:10.1124/dmd.109.031047.

ABBREVIATIONS: UGT, UDP-glucuronosyltransferase; SULT, sulfotransferase; HPLC, high-performance liquid chromatography; DAD, diode array detector; UDPGA, UDP-glucuronic acid; PAPS, 3′-phosphoadenosine 5′-phosphosulfate; DMSO, dimethyl sulfoxide.

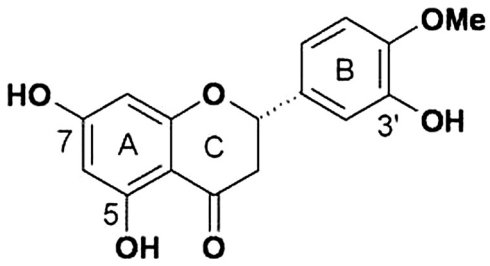

FIG. 1. Chemical structure of hesperetin (4′-methoxy-3′,5,7-trihydroxyflavanone).

UGT2A (UGT2A1, UGT2A2, and UGT2A3), the UGT2B (UGT2B4, UGT2B7, UGT2B10, UGT2B11, UGT2B15, UGT2B17, and UGT2B28), the UGT3 (UGT3A1 and UGT3A2), or the UGT8 (UGT8A1) family (Mackenzie et al., 2005). SULTs form a gene superfamily and a total of 10 different SULT proteins have been detected in human tissues including SULT1A1, SULT1A2, SULT1A3 (encoded by *SULT1A3* and *SULT1A4* and therefore also called SULT1A3/4), SULT1B1, SULT1C2, SULT1C4, SULT1E1, SULT2A1, SULT2B1_v2, and SULT4A1_v2 (Teubner et al., 2007; Riches et al., 2009). In addition, there are some SULTs that have only been detected at the mRNA level: SULT2B1_v1, SULT1C3, and SULT6B1 (Meinl et al., 2008a), the latter solely in testis (Freimuth et al., 2004). SULT1C2, SULT1C4, SULT2B1_v1, SULT2B1_v2, and SULT4A1_v2 are also referred to as SULT1C1, SULT1C2, SULT2B1a, SULT2B1b, and SULT4A1, respectively, in the literature, not following the nomenclature proposed by Blanchard et al. (2004).

We previously characterized the metabolism of hesperetin in vitro using Caco-2 cell monolayers as a model for the small intestinal barrier and reported that hesperetin is metabolized into 7-*O*-glucuronide and 7-*O*-sulfate metabolites (Brand et al., 2008). However, analysis of metabolites in plasma demonstrated the existence of other glucuronide and sulfo-conjugates as well (Matsumoto et al., 2004; Mullen et al., 2008; Brett et al., 2009). Different individual UGTs and SULTs probably possess different kinetics and regioselectivity for the conjugation of hesperetin, as has been reported for the glucuronidation and sulfonation of other flavonoids (Boersma et al., 2002; Otake et al., 2002; Zhang et al., 2007a; Tang et al., 2009), and, therefore, different levels of expression of UGTs and SULTs might lead to different metabolite patterns.

In the present article, we determined the kinetics for the conversion of hesperetin into glucuronidated and sulfonated metabolites by individual UGT and SULT enzymes, respectively. The metabolites formed were identified by HPLC-DAD in combination with authentic standards or ^{1}H NMR. The UGT isoforms tested include 12 individual UGTs reported to be expressed, at least at the mRNA level, in human intestinal and hepatic cells: UGT1A1, UGT1A3, UGT1A4, UGT1A6, UGT1A7, UGT1A8, UGT1A9, UGT1A10, UGT2B4, UGT2B7, UGT2B15, and UGT2B17 (Gregory et al., 2004; Nakamura et al., 2008; Izukawa et al., 2009; Ohno and Nakajin, 2009). The SULT isoforms tested include 12 individual SULTs, which have been detected in human intestinal and hepatic tissues: SULT1A1, SULT1A2, SULT1A3, SULT1B1, SULT1C2, SULT1E1, SULT1C4, and SULT2A1 (Teubner et al., 2007; Meinl et al., 2009; Riches et al., 2009) and in addition SULT1C3, SULT2B1_v1, SULT2B1_v2, and SULT4A1_v2, which have not been detected on the protein level in these tissues (Meinl et al., 2008a,b).

Furthermore, we studied the apparent kinetics of glucuronidation and sulfonation using, respectively, microsomes and cytosol derived from tissues from human and rat playing a role during the first-pass metabolism of hesperetin after ingestion of hesperidin or hesperetin 7-*O*-glucoside: the small intestine, the colon, and the liver.

Materials and Methods

Materials. Alamethicin (from *Trichoderma viride*), hesperetin (purity ≥95%), L-ascorbic acid, and UDP-glucuronic acid (UDPGA) were obtained from Sigma-Adlrich (St. Louis, MO), 3′-phosphoadenosine 5′-phosphosulfate (PAPS) was from Fluka (Buchs, Switzerland), deuterated acetic acid, dimethyl sulfoxide (DMSO), dipotassium hydrogen phosphate trihydrate, hydrochloric acid, and potassium dihydrogen phosphate were from Merck (Darmstadt, Germany), acetonitrile and methanol were from Sigma-Aldrich (Steinheim, Germany), Tris was from Invitrogen (Carlsbad, CA), and trifluoroacetic acid was from Mallinckrodt Baker (Phillipsburg, NJ). Deuterated methanol-d4 (99.96% d) was obtained from Euriso-Top (Gif-sur-Yvette, France). Authentic standards of hesperetin 7-*O*-glucuronide (purity >90%), hesperetin 3′-*O*-glucuronide (purity >90%), and hesperetin 7-*O*-sulfate (purity <50%) were provided by the Nestlé Research Center (Lausanne, Switzerland).

UGT Supersomes from cDNA-transfected insect cells expressing individual human UGTs were obtained from BD Gentest (Woburn, MA), and their glucuronidation activities toward standard substrates as described by the supplier were as follows: UGT1A1 (lot 95244) and UGT1A3 (lot 70200), 817 and 190 pmol min^{-1} mg of protein^{-1} estradiol 3-glucuronidation activity, respectively; UGT1A4 (lot 95375), 1100 pmol min^{-1} mg of protein^{-1} trifluoperazine glucuronidation activity; UGT1A6 (lot 70201), UGT1A7 (lot 68106), UGT1A8 (lot 95862), UGT1A9 (lot 81291), UGT1A10 (lot 96097), UGT2B4 (lot 93808), UGT2B7 (lot 83494), and UGT2B15 (lot 70203), 5200, 12,000, 630, 7200, 86, 180, 1200, and 3000 pmol min^{-1} mg of protein^{-1} 7-hydroxy 4-trifluoromethylcoumarin glucuronidation activity, respectively; and UGT2B17 (lot 09302), 1100 pmol min^{-1} mg of protein^{-1} eugenol glucuronidation activity. SULTs from cDNA-transfected bacteria expressing quantified concentrations of individual human SULT enzymes were prepared as described elsewhere in detail (Meinl et al., 2006).

Pooled human small intestinal microsomes (batch MIC318012), pooled rat (male Sprague-Dawley) small intestinal microsomes (batch MIC323019), pooled human small intestinal cytosol (batch CYT318004), and pooled rat (male Sprague-Dawley) small intestinal cytosol (batch CYT323008) were obtained from Biopredic (Rennes, France), without quantified glucuronidation or sulfonation activities. Human single-donor colon microsomes from a 64-year-old male (batch MIC317008), pooled colon microsomes from rat (male Sprague-Dawley) (batch MIC322003), human single-donor colon cytosol from a 64-year-old male (batch CYT317005), and pooled colon cytosol from rat (male Sprague-Dawley) (batch CYT322003) were provided by Biopredic, without quantified glucuronidation or sulfonation activities. Ethical permission for the use of the human tissue extract was obtained by Biopredic. Pooled human liver microsomes (lot 28831) with 920 pmol min^{-1} mg of protein^{-1} estradiol 3-glucuronidation activity, 890 pmol min^{-1} mg of protein^{-1} trifluoperazine glucuronidation activity, and 2400 pmol min^{-1} mg of protein^{-1} propofol glucuronidation activity, pooled rat (male Sprague-Dawley) liver microsomes (lot 83481) without quantified glucuronidation activity, and pooled human liver cytosol (lot 99925) and pooled rat (male Sprague-Dawley) liver cytosol (lot 08003) with 320 and 1900 pmol min^{-1} mg of protein^{-1} 7-hydroxycoumarin sulfotransferase activity, respectively, as described by the supplier, were provided by BD Gentest.

Incubations with UGTs or Rat or Human Microsomes. To study glucuronidation of hesperetin by individual UGTs or microsomal preparations, incubation mixtures (total volume 200 μl) were

prepared containing 10 mM $MgCl_2$, 25 μg/ml alamethicin added from a 200× concentrated stock solution in methanol (final concentration 0.5% methanol), 0.1, 0.2, or 0.5 mg/ml protein, and 1 mM UDPGA in 50 mM Tris-HCl (pH 7.5) (Boersma et al., 2002). The reaction was started by addition of hesperetin from a 200× concentrated stock solution in DMSO (final concentration 0.5% DMSO) and incubated for 5 min (UGT1A10, UGT2B7, and human and rat liver microsomes), 10 min (UGT1A1, UGT1A3, UGT1A7, UGT1A8, UGT1A9, UGT2B15, and human and rat small intestinal microsomes), 15 min (human and rat colon microsomes), or 30 min (UGT1A4, UGT1A6, UGT2B4, and UGT2B17) at 37°C. The final concentration series was 1, 2.5, 5, 10, 15, 25, 35, and 50 μM (n = 1–2) or 2.5, 5, 10, 15, 25, and 50 μM (n = 1–3) hesperetin for all UGTs tested. The reaction was terminated by addition of 50 μl of acetonitrile. Under these conditions metabolite formation was linear in time and with the amount of protein added (data not shown). Activity is expressed in nanomoles per minute per milligram of protein.

Incubations with SULTs or Rat or Human Cytosol. To study sulfonation of hesperetin, incubation mixtures (total volume 100 μl) were prepared containing 5 mM $MgCl_2$, 100 μM PAPS, and 0.04 to 0.23 mg/ml protein (cytosol), or 0.03 to 0.1 mg/ml protein (individual SULTs) in 50 mM potassium phosphate (pH 7.4). The reaction was started by addition of hesperetin (final concentration series was 1, 2.5, 5, 10, 15, 25, 35, and 50 μM hesperetin) from a 100-fold concentrated stock solution in DMSO (final concentration 1% DMSO) and incubated for 3 min (SULT1A1, SULT1A2, SULT1C4, and human and rat liver cytosol), 5 min (SULT1E1 and human small intestinal cytosol), 9 min (SULT1A3), 10 min (SULT1B1), 90 min (human colon cytosol), 120 min (SULT1C2 and SULT2A1), 150 min (rat small intestinal and colon cytosol), or 180 min (SULT1C3, SULT2B1_v1, SULT2B1_v2, and SULT4A1_v2) at 37°C. Because SULT1A1, SULT1A2, SULT1C4, SULT1E1, and some cytosolic fractions showed substrate inhibition at concentrations >1, >1, and >3 μM, respectively, additional series of 0.1, 0.15, 0.25, 0.35, 0.5, 0.75, 1, and 1.5 μM hesperetin (SULT1A1, SULT1A2, and SULT1C4), or a series of 0.1, 0.25, 0.5, 0.75, 1, 1.5, 2.5, and 3.5 μM hesperetin (SULT1E1 and cytosolic fractions) were used. The reaction was terminated by addition of 25 μl of acetonitrile. Under these conditions metabolite formation was linear with time and the amount of protein added (data not shown). Activity is expressed in nanomoles per minute per milligram of protein for the cytosolic fractions and in nanomoles per minute per milligram of SULT protein for the individual SULTs (Meinl et al., 2006).

Enzyme Kinetics. To determine the kinetics for glucuronidation and sulfonation, incubations were performed as described above. The maximum velocity (V_{max}) and Michaelis-Menten constant (K_m) for the formation of the different phase II metabolites of hesperetin were determined by fitting the data to the Michaelis-Menten steady-state model $v = V_{max}/(1 + (K_m/[S]))$, with $[S]$ being the hesperetin concentration, using the LSW data analysis toolbox (version 1.1.1; MDL Information Systems, San Ramon, CA). For reactions demonstrating substrate inhibition, the V_{max}, K_m, and inhibition constant (K_i) were determined by fitting the data to the substrate inhibition equation $v = V_{max} \times [S]/[K_m + [S] \times (1 + [S]/K_i)]$ using GraphPad Prism (version 5.02; GraphPad Software Inc., San Diego, CA).

HPLC Analysis. To analyze the formation of hesperetin metabolites in the enzymatic incubations, reaction mixtures were centrifuged for 4 min at 16,000g and samples of 50 μl of the supernatant were injected onto a Alliance 2695 separation module (Waters, Milford, MA) connected to a 2996 DAD (Waters) with an Alltima C18 5-μm 150 × 4.6 mm column with 7.5 × 4.6 mm guard column (Alltech, Breda, The Netherlands). Elution was at a flow rate of 1 ml/min. The gradient for the analysis of samples from the incubations with cytosol or SULTs started at 0% acetonitrile in nanopure water containing 0.1% trifluoroacetic acid, increasing to 10% acetonitrile in 5 min, to 15% in the following 16 min, to 50% in the next 16 min, and to 80% in 1 min, followed by a cleaning and reequilibration step. The gradient to analyze the samples from the incubations with microsomes or UGTs started at 0% acetonitrile in nanopure water containing 0.1% trifluoroacetic acid, increasing to 25% acetonitrile in 10 min, which condition was kept for 21 min, whereafter the percentage of acetonitrile was increased to 60% in 7 min and to 80% in 1 min, followed by a cleaning and reequilibration step. DAD-UV spectra were recorded between 200 and 420 nm, and chromatograms acquired at 280 nm were used for presentation and quantification.

Metabolite Identification and Quantification. Hesperetin 7-*O*-glucuronide, hesperetin 3′-*O*-glucuronide, and hesperetin 7-*O*-sulfate were identified using authentic standards by their HPLC-DAD retention times and UV spectra. With use of the HPLC gradient for analysis of the samples from the glucuronidation reactions, the retention times were as follows: hesperetin, 37.2 min (UV_{max} = 285.9 nm); hesperetin 7-*O*-glucuronide, 17.7 min (UV_{max} = 285.9 nm); and hesperetin 3′-*O*-glucuronide, 18.5 min (UV_{max} = 285.9 nm). With use of the HPLC gradient for the analysis of the samples from the sulfonation reactions, the retention times were as follows: hesperetin, 36.7 min (UV_{max} = 285.9 nm) and hesperetin 7-*O*-sulfate, 31.6 min (UV_{max} = 281.2 nm, shoulder at 338 nm). Another metabolite resulting from the cytosolic and SULT incubations with PAPS at a retention time of 30.7 min (UV_{max} = 290.7 nm) was repeatedly collected during HPLC-DAD separation, freeze-dried, and resolved in acidified, deuterated methanol for ^{1}H-NMR analysis. ^{1}H-NMR analysis revealed this metabolite to be hesperetin 3′-*O*-sulfate (for details, see *Results*). Hesperetin 7-*O*-glucuronide and hesperetin 3′-*O*-glucuronide were quantified on the basis of a calibration curve made with authentic standards. Hesperetin 7-*O*-sulfate and hesperetin 3′-*O*-sulfate were quantified indirectly using the calibration curve for hesperetin, and multiplication factors were determined by enzymatic hydrolysis of hesperetin 7-*O*-sulfate (factor 1.27) and hesperetin 3′-*O*-sulfate (factor 0.86) into unconjugated hesperetin, which could be quantified with a calibration curve.

^{1}H NMR Analysis. ^{1}H NMR analysis was performed using an Avance III 600 MHz (Bruker, Ettlingen, Germany) with cryoprobe. A Noesygppr1d pulse sequence with 3-s delay, 0.1-s mixing time, and 1.8-s acquisition time was used (18,028 Hz sweep width; 64 K data points). Spectra were obtained at 25°C. Resonances are reported relative to methanol-d4 at 3.34 ppm.

Results

Identification of Hesperetin Metabolites. Figure 2 depicts part of a chromatogram from the HPLC-DAD analysis of the supernatant of an incubation of hesperetin with UGT1A9 and UDPGA. Two metabolites were formed and identified as hesperetin 7-*O*-glucuronide (t_R, 17.7 min; UV_{max}, 285.9 nm) and hesperetin 3′-*O*-glucuronide (t_R, 18.5 min; UV_{max}, 285.9 nm) on the basis of analysis of the corresponding authentic metabolite standards. Figure 3 depicts part of a chromatogram from the HPLC-DAD analysis of the supernatant from an incubation of hesperetin with SULT1A3 and PAPS. Two metabolites were formed, one of which was identified as hesperetin 7-*O*-sulfate (t_R, 31.6 min; UV_{max}, 281.2 nm, shoulder at 338 nm) on the basis of analysis of the corresponding authentic metabolite standard. The fraction containing the second metabolite (t_R, 30.7 min; UV_{max}, 290.7 nm), which could not be identified with the available authentic standards, was collected, freeze-dried, dissolved in acidified methanol, and analyzed by ^{1}H-NMR.

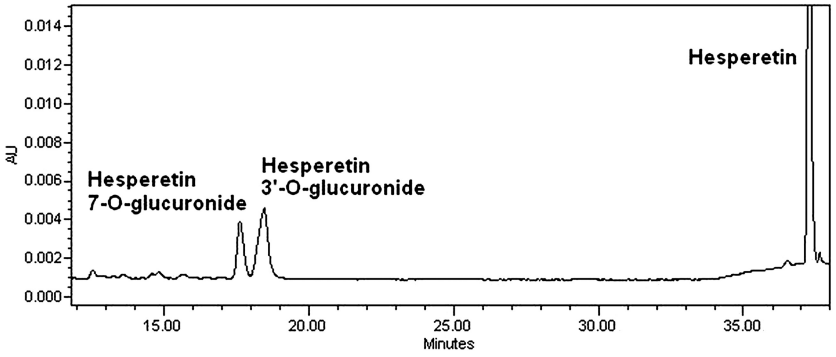

FIG. 2. Representative section of the HPLC chromatogram of the supernatant from the incubation of hesperetin with UGT1A9 and UDPGA showing the hesperetin glucuronide conjugates. AU, absorbance units.

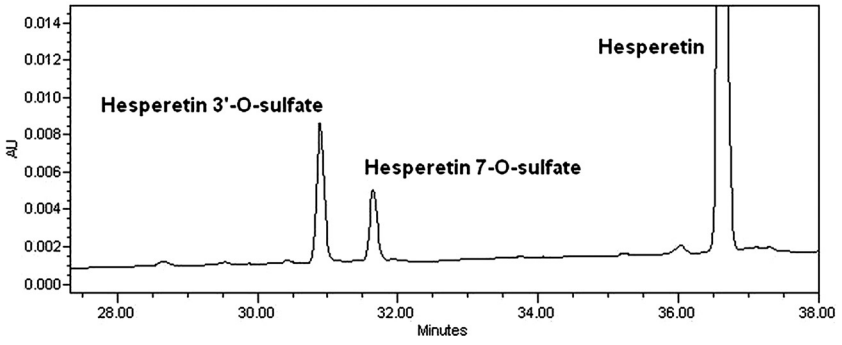

FIG. 3. Representative section of the HPLC chromatogram of the supernatant from the incubation of hesperetin with SULT1A3 and PAPS showing the hesperetin sulfo-conjugates. AU, absorbance units.

TABLE 1

^{1}H NMR data of hesperetin and the metabolite (identified as hesperetin 3′-O-sulfate) formed in the incubation mixture of hesperetin with specific SULT isoforms and human small intestinal cytosol and PAPS

The differences in chemical shift values of the protons in the metabolite compared with the chemical shift values of the same protons in hesperetin are given in parentheses.

Compound	H6	H8	H3 a	H3 b	H2	H2′	H5′	H6′
Hesperetin								
^{1}H NMR chemical shift (ppm)	5.91	5.95	3.11	2.74	5.36	6.98	6.96	6.94
J (Hz)	2.2	2.2	17.0; 12.9	17.0; 3.0	12.9; 3.0	1.7	8.4	1.7; 8.4
Peak splitting	d	d	dd	dd	dd	d	d	dd
Metabolite								
^{1}H NMR chemical shift (ppm)	5.91	5.95	3.10 (−0.01)	2.80 (+0.06)	5.41 (+0.05)	7.64 (+0.66)	7.08 (+0.12)	7.27 (+0.33)
J (Hz)	2.1	2.1	17.1; 12.9	17.1; 3.0	12.9; 3.0	2.1	8.4	2.1; 8.4
Peak splitting	d	d	dd	dd	dd	d	d	dd

d, doublet; dd, doublet of doublets.

Modern NMR instruments with dedicated cryoprobes provide excellent sensitivity with relatively small amounts of material, provided that this material is of high purity. The sample analyzed contained approximately 0.5 nmol (150 ng) of the unknown sulfonated metabolite. Table 1 summarizes the ^{1}H NMR data for this unknown sulfonated hesperetin metabolite as well as that of the parent compound hesperetin. Comparison of the chemical shift values and *J* values of the corresponding protons in hesperetin and in the unknown sulfonated hesperetin metabolite reveals changes, especially in the ^{1}H NMR data of the protons of the B-ring upon conjugate formation: a relative shift of +0.66 ppm for H2′ and a relative shift of +0.33 ppm for H6′ (Table 1). This result indicates a modification of the hydroxyl moiety at C3′, resulting in a relatively large change in the chemical shift values of the protons H2′ and H6′ at the positions *ortho* and *para* with respect to the modified hydroxyl moiety and is in line with earlier ^{1}H NMR studies on metabolites of quercetin (van der Woude et al., 2004). The signals of the protons H6 and H8 remained unchanged, excluding modification of the other hydroxyl-groups at position 5 or 7 of the hesperetin molecule. Together these data identify the unknown metabolite as hesperetin 3′-*O*-sulfate.

Glucuronidation by Individual UGT Enzymes. Glucuronidation of hesperetin was characterized using human recombinant UGT enzymes. The V_{max} and K_m values obtained for the formation of hesperetin 7-*O*-glucuronide and hesperetin 3′-*O*-glucuronide by the various UGT enzymes are shown in Table 2, as well as the catalytic efficiencies (V_{max}/K_m) derived from these values. The results reveal that hesperetin is most efficiently glucuronidated by UGT1A9. The efficiency of glucuronidation (V_{max}/K_m) decreases in the order of UGT1A9 > UGT1A1 > UGT1A7 > UGT1A3 > UGT1A8 > UGT1A10 > UGT2B7 = UGT2B15 > UGT2B4. The rate of formation of hesperetin 7-*O*-glucuronide by UGT1A6 was virtually linear with the applied concentration: 0.018 nmol min^{-1} mg of protein^{-1} 7-*O*-glucuronide formed per micromole of hesperetin, which excluded determination of the kinetic parameters V_{max} and K_m by fitting the data to the Michaelis-Menten equation. Higher doses of hesperetin could not be tested because of the limited solubility of hesperetin in aqueous solutions. The enzymes

TABLE 2

V_{max} and K_m values determined from three to four independent curves and the catalytic efficiencies (V_{max}/K_m) derived from these values, for the glucuronidation of hesperetin (1 up to 50 μM) by individual UGT enzymes

Data are means ± S.E.M.

UGT Isoform	7-*O*-Glucuronidation			3′-*O*-Glucuronidation		
	K_m	V_{max}	V_{max}/K_m	K_m	V_{max}	V_{max}/K_m
	μM	*nmol min^{-1} mg protein^{-1}*	*μl min^{-1} mg protein^{-1}*	*μM*	*nmol min^{-1} mg protein^{-1}*	*μl min^{-1} mg protein^{-1}*
UGT1A1	4.0 ± 1.3	1.35 ± 0.29	339	1.2 ± 0.5	0.46 ± 0.06	376
UGT1A3	16.5 ± 4.6	3.94 ± 0.74	239	N.D.	N.D.	
UGT1A4	N.D.[a]	N.D.[a]	—[a]	N.D.	N.D.	
UGT1A6	—[b]	—[b]	18[b]	N.D.	N.D.	
UGT1A7	105 ± 67.9	0.47 ± 0.04	5	8.7 ± 1.6	2.47 ± 0.63	285
UGT1A8	63.3 ± 11.8	2.33 ± 1.20	37	19.2 ± 3.9	3.18 ± 1.78	166
UGT1A9	5.3 ± 0.8	2.19 ± 0.10	411	4.0 ± 0.3	3.89 ± 0.20	981
UGT1A10	30.4 ± 8.2	2.82 ± 0.69	93	31.2 ± 12.6	0.89 ± 0.29	28
UGT2B4	119 ± 43.7	0.42 ± 0.09	4	N.D.	N.D.	
UGT2B7	53.9 ± 17.6	1.53 ± 0.25	28	42.4 ± 13.9	0.88 ± 0.23	21
UGT2B15	34.5 ± 1.6	0.28 ± 0.01	8	29.9 ± 0.3	1.19 ± 0.02	40
UGT2B17	N.D.[c]	N.D.[c]	—[c]	N.D.[c]	N.D.[c]	—[c]

N.D., not detectable.

[a] UGT1A4 very poorly glucuronidated hesperetin into solely hesperetin 7-*O*-glucuronide, only measurable at the highest test concentration (50 μM), precluding determination of kinetics.

[b] Conjugation velocity by UGT1A6 of hesperetin into hesperetin 7-*O*-glucuronide occurred in a linear manner with dose (0.018 nmol min^{-1} mg of protein^{-1} μmol of hesperetin^{-1}), precluding determination of the individual Michaelis-Menten parameters V_{max} and K_m, but allowing the definition of the catalytic efficiency because the slope of the linear relationship between the rate of formation as a function of the substrate concentration equals V_{max}/K_m.

[c] UGT2B17 very poorly glucuronidated hesperetin, only measurable at the highest test concentrations (50 μM).

UGT1A4 and UGT2B17 demonstrated only very poor glucuronidation activity toward hesperetin under the conditions used in this study, precluding determination of the kinetics. Figure 4 presents an overview of the regioselectivity of the glucuronidation of hesperetin by the individual UGTs at a concentration of 10 μM hesperetin. For all UGTs, the regioselectivity at 1 or 50 μM hesperetin was similar to that obtained at 10 μM. UGT1A3, UGT1A6, and UGT2B4 catalyze glucuronidation specifically at the hydroxyl moiety at C7 of hesperetin, whereas UGT1A7 almost solely conjugated the hydroxyl moiety at C3′. UGT1A1, UGT1A10, and UGT2B7 converted hesperetin into both hesperetin 3′-*O*-glucuronide and hesperetin 7-*O*-glucronide, however preferentially into the latter, whereas UGT1A8, UGT1A9, and UGT2B15 preferentially conjugated the hydroxyl moiety of hesperetin at position 3′. Overall, relatively more hesperetin 7-*O*-glucuronide is formed at higher substrate concentrations (Table 2).

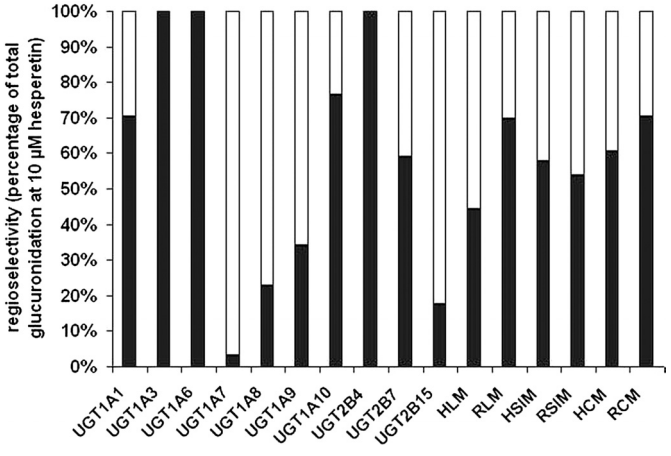

FIG. 4. Regioselectivity of the glucuronidation of hesperetin at position 7 (■) or position 3′ (□) by different UGT enzymes and human and rat microsomes expressed as percentage of the total amount of hesperetin glucuronides formed at a 10 μM hesperetin concentration. HLM, human liver microsomes; RLM, rat liver microsomes; HSIM, human small intestinal microsomes; RSIM, rat small intestinal microsomes; HCM, human colon microsomes; RCM, rat colon microsomes.

Sulfonation by Individual SULT Enzymes. The V_{max} and K_m values determined for the formation of hesperetin 7-*O*-sulfate and hesperetin 3′-*O*-sulfate by individual human SULTs are shown in Table 3, as well as the catalytic efficiencies (V_{max}/K_m) derived from these values. SULT1A1 demonstrated strong substrate inhibition at hesperetin concentrations >0.15 μM, precluding determination of kinetic parameters. The high rate of 3′-*O*-sulfonation up to 117 nmol min^{-1} mg of SULT1A1^{-1} (at 0.15 μM hesperetin) indicates that SULT1A1-mediated sulfonation could probably play an important role in the conjugation of hesperetin at low concentrations. SULT1A2, SULT1C4, and SULT1E1 also demonstrated substrate inhibition at concentrations >1, >1, and >3 μM, respectively. The catalytic efficiency of sulfonation (V_{max}/K_m) of the SULTs (other than SULT1A1) decreases in the order of SULT1C4 > SULT1A2 > SULT1E1 > SULT1A3 > SULT1B1 > SULT1C2 > SULT2A1. The isoenzymes SULT1C3, SULT2B1_v1, SULT2B1_v2, and SULT4A1_v2 did not show any sulfonation activity toward hesperetin under the conditions used in this study. SULT1C4 and SULT2A1 selectively catalyzed the sulfonation at the hydroxyl moiety of position 7 of hesperetin, whereas SULT1A1, SULT1A2, and SULT1E1 solely conjugated the hydroxyl moiety at position 3′ (Fig. 5). SULT1C2 converted hesperetin into both hesperetin 3′-*O*-sulfate and hesperetin 7-*O*-sulfate, however preferentially into the latter, whereas SULT1A3 and SULT1B1 preferentially conjugated the hydroxyl moiety of hesperetin at position 3′ (Fig. 5). For all SULTs, the regioselectivity at 1 or 50 μM hesperetin was similar to that obtained at 10 μM.

Glucuronidation by Human and Rat Tissue Samples. The apparent V_{max} and K_m values for the formation of hesperetin 7-*O*-glucuonide and hesperetin 3′-*O*-glucuronide by human and rat microsomal fractions from different tissues are shown in Table 4, as well as the apparent catalytic efficiencies (V_{max}/K_m) derived from these values. Hesperetin was converted into both glucuronide metabolites by microsomes from all human and rat tissues tested. Generally, the affinity was higher (K_m lower) for glucuronidation at position 3′, whereas the capacity (V_{max}) was higher for glucuronidation at position 7 (Table 4), and, as a result, at higher hesperetin concentrations

TABLE 3

V_{max} and K_m values determined from three independent curves and the catalytic efficiencies (V_{max}/K_m) derived from these values for the sulfonation of hesperetin (1 up to 50 μM unless stated otherwise) by individual SULT enzymes

Data are means ± S.E.M.

SULT Isoform	7-*O*-Sulfonation			3′-*O*-Sulfonation		
	K_m	V_{max}	V_{max}/K_m	K_m	V_{max}	V_{max}/K_m
	μM	*nmol min^{-1} mg protein^{-1}*	*μl min^{-1} mg protein^{-1}*	*μM*	*nmol min^{-1} mg protein^{-1}*	*μl min^{-1} mg protein^{-1}*
SULT1A1	N.D.	N.D.		<0.15[a]	—[a]	—[a]
SULT1A2	N.D.	N.D.		0.5 ± 0.2[b]	454 ± 94.8[b]	881,553[b]
SULT1A3	12.5 ± 3.3	89.9 ± 7.43	7178	13.2 ± 3.0	276 ± 24.8	20,964
SULT1B1	3.9 ± 0.5	3.54 ± 0.66	899	4.3 ± 0.2	21.5 ± 2.14	5003
SULT1C2	66.7 ± 16.1	18.8 ± 6.83	282	28.3 ± 14.5	1.45 ± 0.46	51
SULT1C3	N.D.	N.D.		N.D.	N.D.	
SULT1C4	0.1 ± 0.0[c]	87.4 ± 8.13[c]	1,117,263[c]	N.D.	N.D.	
SULT1E1	N.D.	N.D.		2.5 ± 1.0[d]	538 ± 134[d]	219,242[d]
SULT2A1	80.2 ± 21.0	10.2 ± 1.96	127	N.D.	N.D.	
SULT2B1_v1	N.D.	N.D.		N.D.	N.D.	
SULT2B1_v2	N.D.	N.D.		N.D.	N.D.	
SULT4A1_v2	N.D.	N.D.		N.D.	N.D.	

N.D., not detectable.
[a] SULT1A1 demonstrated strong substrate inhibition at concentrations >0.1 μM, precluding determination of kinetic parameters.
[b] SULT1A2 showed substrate inhibition at concentrations >1 μM hesperetin; K_i = 1.9 μM.
[c] SULT1C4 showed substrate inhibition at concentrations >1 μM hesperetin; K_i = 23.5 μM.
[d] SULT1E1 showed substrate inhibition at concentrations >3 μM hesperetin; K_i = 12.9 μM.

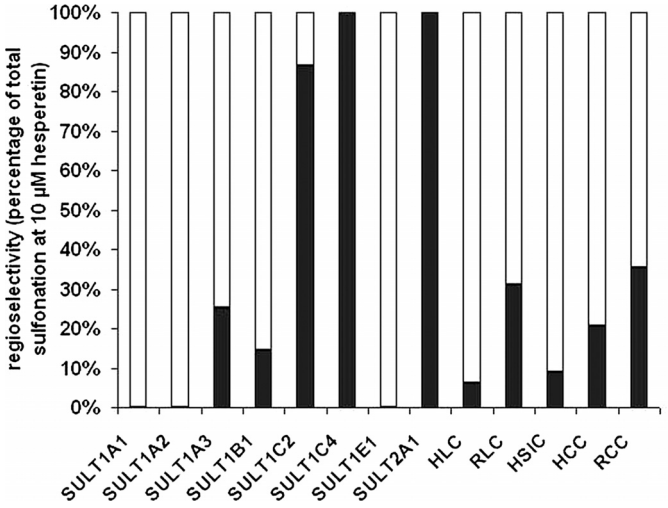

FIG. 5. Regioselectivity of the sulfonation of hesperetin at position 7 (■) or position 3′ (□) by different SULT enzymes and human and rat cytosol expressed as percentage of the total amount of hesperetin sulfates formed at a 10 μM hesperetin concentration. HLC, human liver cytosol; RLC, rat liver cytosol; HSIC, human small intestinal cytosol; HCC, human colon cytosol; RCC, rat colon cytosol.

relatively more hesperetin 7-*O*-glucuronide than hesperetin 3′-glucuronide is formed.

Sulfonation by Human and Rat Tissue Samples. The apparent V_{max} and K_m values determined for the formation of hesperetin 7-*O*-sulfate and hesperetin 3′-*O*-sulfate by human and rat cytosol from different tissues are shown in Table 4, as well as the apparent catalytic efficiencies (V_{max}/K_m) derived from these values. Hesperetin was predominantly converted into hesperetin 3′-*O*-sulfate by human small intestinal cytosol with a K_m of 0.6 μM and a capacity of 0.79 nmol min^{-1} mg of protein^{-1}, whereas rat small intestinal cytosol did not show sulfonation activity toward hesperetin (Table 4). Rat as well as human colonic cytosol showed low catalytic efficiencies. Liver cytosol of both species converted hesperetin into hesperetin 3′-*O*-sulfate already at low concentrations and demonstrated substrate inhibition at hesperetin concentrations >0.25 μM. It is remarkable that rat liver cytosol also demonstrated efficient conversion of hesperetin into hesperetin 7-*O*-sulfate at low concentrations, with substrate inhibition at hesperetin concentrations >0.25 μM, whereas the sample of human liver cytosol demonstrated very little 7-*O*-sulfate formation (Table 4).

Discussion

In the present study, the kinetics for the conjugation of hesperetin by individual UGT and SULT enzymes and rat or human microsomes and cytosol from small intestine, colon, and liver was characterized. Hesperetin was conjugated at the C7 and C3′ hydroxyl moieties. It is interesting to note that conjugation at the C5 hydroxyl moiety was not catalyzed. This phenomenon can be explained by the strong intramolecular hydrogen bond between this hydroxyl moiety and the C4 carbonyl moiety preventing the phase II conjugation (Exarchou et al., 2002). Of all UGTs tested, UGT1A9, UGT1A1, UGT1A7, UGT1A3, and UGT1A8 demonstrated the highest catalytic efficiencies (Table 2). These UGTs have been reported to efficiently catalyze the glucuronidation of other flavonoids as well, as was recently reviewed Zhang et al. (2007b), although the relative efficiency of different UGTs seems to be highly dependent on the flavonoid structure involved. Hesperetin, as other flavonoids, seems not to be a suitable substrate for UGT1A4 (Walle et al., 2000; Boersma et al., 2002; Tang et al., 2009). The regioselectivity of hesperetin glucuronidation varied enzyme specifically (Fig. 4). Differences in the regioselectivity of the flavonoid conjugation by different individual UGTs has also been reported for the conjugation of other flavonoids (Boersma et al., 2002; Otake et al., 2002; Zhang et al., 2007a; Tang et al., 2009), the regioselectivity being dependent on the isoenzyme involved, the flavonoid converted, and the substrate concentration. For instance, luteolin (3′,4′,5,7-tetrahydroxyflavone) was almost solely (98% of HPLC chromatogram peak area) converted into a 7-*O*-glucuronide metabolite by UGT1A6, whereas quercetin (3,3′,4′,5,7-tetrahydroxyflavone), bearing one extra hydroxyl moiety, was metabolized into its 4′-*O*-glucuronide (32%), 7-*O*-glucuronide (30%), 3′-*O*-glucuronide (22%), and 3-*O*-glucuronide (16%) by UGT1A6 (Boersma et al., 2002).

Of the SULT enzymes (apart from SULT1A1), SULT1A2, SULT1C4, and to a lesser extent SULT1E1 and SULT1A3 demonstrated the highest catalytic efficiencies for the sulfonation of

TABLE 4

Apparent V_{max} and K_m values determined from two to three independent curves of the glucuronidation or sulfonation of hesperetin (up to 50 μM unless stated otherwise) by microsomes or cytosol, respectively, from human and rat tissue fractions

Data are means ± S.E.M.

	7-*O*-Glucuronidation			3′-*O*-Glucuronidation			7-*O*-Sulfonation			3′-*O*-Sulfonation		
	K_m(app)	V_{max}(app)	V_{max}(app)/K_m(app)	K_m(app)	V_{max}(app)	V_{max}(app)/K_m(app)	K_m(app)	V_{max}(app)	V_{max}(app)/K_m(app)	K_m(app)	V_{max}(app)	V_{max}(app)/K_m(app)
	μM	*nmol min^{-1} mg protein^{-1}*	*μl min^{-1} mg protein^{-1}*	*μM*	*nmol min^{-1} mg protein^{-1}*	*μl min^{-1} mg protein^{-1}*	*μM*	*nmol min^{-1} mg protein^{-1}*	*μl min^{-1} mg protein^{-1}*	*μM*	*nmol min^{-1} mg protein^{-1}*	*μl min^{-1} mg protein^{-1}*
Small intestine												
Human	8.3 ± 1.9	3.80 ± 0.50	458	6.4 ± 1.2	2.49 ± 0.49	391	9.1 ± 1.5	0.14 ± 0.04	16	0.6 ± 0.2	0.79 ± 0.14	1240
Rat	15.3 ± 3.8	9.85 ± 0.70	643	7.7 ± 0.6	5.91 ± 0.71	764	N.D.	N.D.		N.D.	N.D.	
Colon												
Human	3.7 ± 0.1	1.55 ± 0.08	415	3.4 ± 0.1	0.99 ± 0.02	294	8.6 ± 0.0	0.07 ± 0.00	8	3.3 ± 0.7[a]	0.20 ± 0.02[a]	61[a]
Rat	10.3 ± 0.0	5.41 ± 0.18	524	2.4 ± 0.0	1.41 ± 0.07	598	1.1 ± 0.4	0.01 ± 0.00	4	7.3 ± 1.1[a]	0.04 ± 0.00[a]	5[a]
Liver												
Human	20.1 ± 1.6	8.00 ± 0.23	398	10.6 ± 1.1	6.96 ± 0.79	657	1.5 ± 0.9	0.02 ± 0.00	15	<0.1[b]	—[b]	—[b]
Rat	24.3 ± 0.4	21.08 ± 0.05	868	5.0 ± 0.1	4.04 ± 0.30	801	<0.25[c]	—[c]	—[c]	<0.25[b]	—[b]	—[b]

N.D., not detectable.

[a] Human and rat colon cytosol showed 3′-*O*-sulfonation substrate inhibition at concentrations >25 and >15 μM, respectively; K_i (human colon cytosol) = 446 μM, and K_i (rat colon cytosol) = 22.2 μM.

[b] Human and rat liver cytosol demonstrated strong 3′-*O*-sulfonation substrate inhibition at concentrations of, respectively, >0.1 and >0.25 μM, precluding determination of kinetic parameters.

[c] Rat liver cytosol demonstrated strong 7-*O*-sulfonation substrate inhibition at concentrations of >0.25 μM, precluding determination of kinetic parameters.

hesperetin (Table 3). SULT1A1, SULT1A3, and SULT1E1 have been reported to sulfonate other flavonoids as well (Otake et al., 2002; Nakano et al., 2004; Ung and Nagar, 2007). In the present study, SULT1A1, SULT1A2, and SULT1E1 solely catalyzed the formation of hesperetin 3′-*O*-sulfate, whereas SULT1C4 and SULT2A1 solely catalyzed the formation of hesperetin 7-*O*-sulfate (Fig. 5). The regioselectivity of flavonoid sulfonation appears to be dependent on the SULT isoenzyme as well as on the flavonoid studied: daidzein (4′,7-dihydroxyisoflavone) and genistein (4′,5,7-trihydroxyisoflavone) were reported to be predominantly sulfated by SULT1A1 at position 7 rather than at position 4′, whereas the hydroxyl moieties at both positions were sulfonated with similar efficiency by SULT1E1 (Nakano et al., 2004). At low concentrations of hesperetin, SULT1A2, SULT1C4, SULT1E1 (Table 3), and especially SULT1A1 demonstrated substrate inhibition. This property of SULTs in the conjugation of flavonoids at low concentrations is also reported for the SULT1A1-mediated sulfonation of daidzein (>1.5 μM) and genistein (>2 μM) (Nakano et al., 2004) and for the SULT1E1-mediated sulfonation of quercetin and chrysin (Ung and Nagar, 2007).

Incubations of hesperetin with human and rat microsomal fractions in the presence of UDPGA resulted in formation of hesperetin 7-*O*-glucuronide and hesperetin 3′-*O*-glucuronide (Table 4). Based on the kinetics of the individual human UGTs (Table 2) and the data on UGT mRNA expression levels (Gregory et al., 2004; Nakamura et al., 2008; Izukawa et al., 2009; Ohno and Nakajin, 2009), the 7-*O*-glucuronidation of hesperetin in human tissue fractions is probably catalyzed by UGT1A1 and UGT1A9. The 3′-*O*-glucuronidation of hesperetin by human microsomes is probably catalyzed by UGT1A9 and UGT1A1, whereas in the human small intestinal and colonic microsomes UGT1A7 and UGT1A8 may contribute as well. However, one should keep in mind that selectivity profiles by single UGTs in complete systems, in which protein-protein interactions may occur, may be different from those in in vitro model systems (Fujiwara et al., 2007). Taking the catalytic efficiencies (Table 2) and the mRNA expression levels of the rat ortholog UGTs into account (Shelby et al., 2003), it can be foreseen that, in rat liver and rat intestinal microsomes, rat UGT1A1 and rat UGT1A7 are probably responsible for the glucuronidation of hesperetin.

Incubations with the human cytosolic fractions demonstrated preferential sulfonation of position 3′ of hesperetin (Table 4). Although SULT1A2, SULT1C4, and SULT1E1 demonstrate high catalytic efficiencies based on expression levels (Teubner et al., 2007; Riches et al., 2009), they are minor SULT isoforms in the intestine and liver. It is concluded that SULT1A1 in particular is involved in the sulfonation of hesperetin in the human liver, whereas SULT1B1 and SULT1A3 will preferably contribute to the intestinal sulfonation of hesperetin. Our incubations with human cytosol demonstrating predominant formation of hesperetin 3′-*O*-sulfate, the major metabolite formed by SULT1A1 as well as by SULT1B1 and SULT1A3, support such a notion. Hesperetin was not sulfonated by rat small intestinal cytosol, which corresponds with the negligible SULT expression in the small intestine of rats (Meinl et al., 2009). The hepatic expression of the rat ortholog of SULT1C4, a form not detected in human liver (Sakakibara et al., 1998), probably explains the formation of hesperetin 7-*O*-sulfate by rat liver cytosol.

When both SULTs and UGTs play a role at the same time, such as in the in vivo situation, the existence of mixed conjugates has been reported as well. In a study in which human volunteers were given up to 1 liter of orange juice providing 444 mg/l hesperidin, the circulating forms of hesperetin in the plasma consisted of

glucuronides (87%) and sulfoglucuronides (13%) as determined after specific enzymatic hydrolysis (Manach et al., 2003). In another study in which human volunteers were given 250 ml of orange juice containing 410 mg/l hesperidin, only hesperetin glucuronides were detected in the plasma; however, substantial amounts of hesperetin sulfoglucuronides were detected in the urine as indicated by liquid chromatography-tandem mass spectrometry (Mullen et al., 2008). The authors argued that the kidney may be involved in postabsorption phase II metabolism, which could be explained by the expression of SULT1A1 in the kidneys (Meinl et al., 2006; Riches et al., 2009), the enzyme for which we found a high affinity toward hesperetin resulting in sulfonation at very low concentrations. In a third study in which human volunteers were given oranges or orange juice providing, respectively, 161 or 145 mg of hesperidin, hesperetin 7-*O*-glucuronide and 3′-*O*-glucuronide were detected in blood and plasma, as well as hesperetin 3′-*O*-sulfate, as qualified by liquid chromatography-tandem mass spectrometry and metal complexation techniques (Brett et al., 2009). The absence of hesperetin 7-*O*-sulfate in these human volunteers is supported by the sulfonation kinetics found in the present study.

We recently analyzed the metabolism of hesperetin in vitro using Caco-2 cell monolayers as a model of the intestinal barrier. After incubations of hesperetin with Caco-2 cell monolayers, formation of hesperetin 7-*O*-glucuronide and 7-*O*-sulfate was observed, whereas no metabolites of hesperetin conjugated at position 3′ were detected. These observations could be explained by the relatively strong expression of SULT1C4 (Tamura et al., 2001; Meinl et al., 2008b) and UGT1A6 (Paine and Fisher, 2000), both enzymes specifically catalyzing the conjugation at position 7, compared with other SULT or UGT forms in Caco-2 cells. Moreover, small interfering RNA-mediated UGT1A6 silencing in this cell line heavily decreased the glucuronidation of the flavonoid apigenin, which demonstrates an important role for UGT1A6 in the glucuronidation by Caco-2 cells of a structurally related compound (Liu et al., 2007).

In conclusion, the results of the present study show that individual UGTs and SULTs demonstrate marked regioselective kinetics for conjugation of hesperetin. As a result, variations in expression levels of these UGTs and SULTs give rise to different metabolite patterns in different biological systems. Because different flavonoid conjugates may have different physiological and/or biological properties, this regioselective conjugation by different UGT and SULT enzymes should not be ignored in flavonoid research. Finally, given the high catalytic efficiency and expression levels of UGTs in intestinal tissue, it can be concluded that first-pass metabolism within the intestinal cells contributes significantly to the formation of hesperetin 3′-*O*-glucuronide and 7-*O*-glucuronide, the major hesperetin metabolites found in vivo.

References

Blanchard RL, Freimuth RR, Buck J, Weinshilboum RM, and Coughtrie MW (2004) A proposed nomenclature system for the cytosolic sulfotransferase (SULT) superfamily. *Pharmacogenetics* **14:**199–211.

Boersma MG, van der Woude H, Bogaards J, Boeren S, Vervoort J, Cnubben NH, van Iersel ML, van Bladeren PJ, and Rietjens IM (2002) Regioselectivity of phase II metabolism of luteolin and quercetin by UDP-glucuronosyl transferases. *Chem Res Toxicol* **15:**662–670.

Brand W, van der Wel PA, Rein MJ, Barron D, Williamson G, van Bladeren PJ, and Rietjens IM (2008) Metabolism and transport of the citrus flavonoid hesperetin in Caco-2 cell monolayers. *Drug Metab Dispos* **36:**1794–1802.

Brett GM, Hollands W, Needs PW, Teucher B, Dainty JR, Davis BD, Brodbelt JS, and Kroon PA (2009) Absorption, metabolism and excretion of flavanones from single portions of orange fruit and juice and effects of anthropometric variables and contraceptive pill use on flavanone excretion. *Br J Nutr* **101:**664–675.

Exarchou V, Nenadis N, Tsimidou M, Gerothanassis IP, Troganis A, and Boskou D (2002) Antioxidant activities and phenolic composition of extracts from Greek oregano, Greek sage, and summer savory. *J Agric Food Chem* **50:**5294–5299.

Freimuth RR, Wiepert M, Chute CG, Wieben ED, and Weinshilboum RM (2004) Human cytosolic sulfotransferase database mining: identification of seven novel genes and pseudogenes. *Pharmacogenomics J* **4:**54–65.

Fujiwara R, Nakajima M, Yamanaka H, Katoh M, and Yokoi T (2007) Interactions between human UGT1A1, UGT1A4, and UGT1A6 affect their enzymatic activities. *Drug Metab Dispos* **35:**1781–1787.

Gregory PA, Lewinsky RH, Gardner-Stephen DA, and Mackenzie PI (2004) Regulation of UDP glucuronosyltransferases in the gastrointestinal tract. *Toxicol Appl Pharmacol* **199:**354–363.

Horcajada MN, Habauzit V, Trzeciakiewicz A, Morand C, Gil-Izquierdo A, Mardon J, Lebecque P, Davicco MJ, Chee WS, Coxam V, et al. (2008) Hesperidin inhibits ovariectomized-induced osteopenia and shows differential effects on bone mass and strength in young and adult intact rats. *J Appl Physiol* **104:**648–654.

Izukawa T, Nakajima M, Fujiwara R, Yamanaka H, Fukami T, Takamiya M, Aoki Y, Ikushiro S, Sakaki T, and Yokoi T (2009) Quantitative analysis of UDP-glucuronosyltransferase (UGT) 1A and UGT2B expression levels in human livers. *Drug Metab Dispos* **37:**1759–1768.

Liu X, Tam VH, and Hu M (2007) Disposition of flavonoids via enteric recycling: determination of the UDP-glucuronosyltransferase isoforms responsible for the metabolism of flavonoids in intact Caco-2 TC7 cells using siRNA. *Mol Pharm* **4:**873–882.

Liu Z and Hu M (2007) Natural polyphenol disposition via coupled metabolic pathways. *Expert Opin Drug Metab Toxicol* **3:**389–406.

Mackenzie PI, Bock KW, Burchell B, Guillemette C, Ikushiro S, Iyanagi T, Miners JO, Owens IS, and Nebert DW (2005) Nomenclature update for the mammalian UDP glycosyltransferase (UGT) gene superfamily. *Pharmacogenet Genomics* **15:**677–685.

Manach C, Morand C, Gil-Izquierdo A, Bouteloup-Demange C, and Rémésy C (2003) Bioavailability in humans of the flavanones hesperidin and narirutin after the ingestion of two doses of orange juice. *Eur J Clin Nutr* **57:**235–242.

Matsumoto H, Ikoma Y, Sugiura M, Yano M, and Hasegawa Y (2004) Identification and quantification of the conjugated metabolites derived from orally administered hesperidin in rat plasma. *J Agric Food Chem* **52:**6653–6659.

Meinl W, Donath C, Schneider H, Sommer Y, and Glatt H (2008a) SULT1C3, an orphan sequence of the human genome, encodes an enzyme activating various promutagens. *Food Chem Toxicol* **46:**1249–1256.

Meinl W, Ebert B, Glatt H, and Lampen A (2008b) Sulfotransferase forms expressed in human intestinal Caco-2 and TC7 cells at varying stages of differentiation and role in benzo[*a*]pyrene metabolism. *Drug Metab Dispos* **36:**276–283.

Meinl W, Pabel U, Osterloh-Quiroz M, Hengstler JG, and Glatt H (2006) Human sulphotransferases are involved in the activation of aristolochic acids and are expressed in renal target tissue. *Int J Cancer* **118:**1090–1097.

Meinl W, Sczesny S, Brigelius-Flohé R, Blaut M, and Glatt H (2009) Impact of gut microbiota on intestinal and hepatic levels of phase 2 xenobiotic-metabolizing enzymes in the rat. *Drug Metab Dispos* **37:**1179–1186.

Mullen W, Archeveque MA, Edwards CA, Matsumoto H, and Crozier A (2008) Bioavailability and metabolism of orange juice flavanones in humans: impact of a full-fat yogurt. *J Agric Food Chem* **56:**11157–11164.

Nakamura A, Nakajima M, Yamanaka H, Fujiwara R, and Yokoi T (2008) Expression of UGT1A and UGT2B mRNA in human normal tissues and various cell lines. *Drug Metab Dispos* **36:**1461–1464.

Nakano H, Ogura K, Takahashi E, Harada T, Nishiyama T, Muro K, Hiratsuka A, Kadota S, and Watabe T (2004) Regioselective monosulfation and disulfation of the phytoestrogens daidzein and genistein by human liver sulfotransferases. *Drug Metab Pharmacokinet* **19:**216–226.

Németh K, Plumb GW, Berrin JG, Juge N, Jacob R, Naim HY, Williamson G, Swallow DM, and Kroon PA (2003) Deglycosylation by small intestinal epithelial cell beta-glucosidases is a critical step in the absorption and metabolism of dietary flavonoid glycosides in humans. *Eur J Nutr* **42:**29–42.

Nielsen IL, Chee WS, Poulsen L, Offord-Cavin E, Rasmussen SE, Frederiksen H, Enslen M, Barron D, Horcajada MN, and Williamson G (2006) Bioavailability is improved by enzymatic modification of the citrus flavonoid hesperidin in humans: a randomized, double-blind, crossover trial. *J Nutr* **136:**404–408.

Ohno S and Nakajin S (2009) Determination of mRNA expression of human UDP-glucuronosyltransferases and application for localization in various human tissues by real-time reverse transcriptase-polymerase chain reaction. *Drug Metab Dispos* **37:**32–40.

Otake Y, Hsieh F, and Walle T (2002) Glucuronidation versus oxidation of the flavonoid galangin by human liver microsomes and hepatocytes. *Drug Metab Dispos* **30:**576–581.

Paine MF and Fisher MB (2000) Immunochemical identification of UGT isoforms in human small bowel and in Caco-2 cell monolayers. *Biochem Biophys Res Commun* **273:**1053–1057.

Riches Z, Stanley EL, Bloomer JC, and Coughtrie MW (2009) Quantitative evaluation of the expression and activity of five major sulfotransferases (SULTs) in human tissues: the SULT "pie." *Drug Metab Dispos* **37:**2255–2261.

Sakakibara Y, Yanagisawa K, Katafuchi J, Ringer DP, Takami Y, Nakayama T, Suiko M, and Liu MC (1998) Molecular cloning, expression, and characterization of novel human SULT1C sulfotransferases that catalyze the sulfonation of *N*-hydroxy-2-acetylaminofluorene. *J Biol Chem* **273:**33929–33935.

Shelby MK, Cherrington NJ, Vansell NR, and Klaassen CD (2003) Tissue mRNA expression of the rat UDP-glucuronosyltransferase gene family. *Drug Metab Dispos* **31:**326–333.

Silberberg M, Morand C, Mathevon T, Besson C, Manach C, Scalbert A, and Remesy C (2006) The bioavailability of polyphenols is highly governed by the capacity of the intestine and of the liver to secrete conjugated metabolites. *Eur J Nutr* **45:**88–96.

Tamura HO, Taniguchi K, Hayashi E, Hiyoshi Y, and Nagai F (2001) Expression profiling of sulfotransferases in human cell lines derived from extra-hepatic tissues. *Biol Pharm Bull* **24:**1258–1262.

Tang L, Singh R, Liu Z, and Hu M (2009) Structure and concentration changes affect characterization of UGT isoform-specific metabolism of isoflavones. *Mol Pharm* **6:**1466–1482.

Teubner W, Meinl W, Florian S, Kretzschmar M, and Glatt H (2007) Identification and localization of soluble sulfotransferases in the human gastrointestinal tract. *Biochem J* **404:**207–215.

Tomás-Barberán FA, and Clifford MN (2000) Flavanones, chalcones and dihydrochalcones—nature, occurrence and dietary burden. *J Sci Food Agric* **80:**1073–1080.

Ung D and Nagar S (2007) Variable sulfation of dietary polyphenols by recombinant human sulfotransferase (SULT) 1A1 genetic variants and SULT1E1. *Drug Metab Dispos* **35:**740–746.

van der Woude H, Boersma MG, Vervoort J, and Rietjens IM (2004) Identification of 14 quercetin phase II mono- and mixed conjugates and their formation by rat and human phase II in vitro model systems. *Chem Res Toxicol* **17:**1520–1530.

Walle T, Otake Y, Galijatovic A, Ritter JK, and Walle UK (2000) Induction of UDP-glucuronosyltransferase UGT1A1 by the flavonoid chrysin in the human hepatoma cell line hep G2. *Drug Metab Dispos* **28:**1077–1082.

Zhang L, Lin G, and Zuo Z (2007a) Involvement of UDP-glucuronosyltransferases in the extensive liver and intestinal first-pass metabolism of flavonoid baicalein. *Pharm Res* **24:**81–89.

Zhang L, Zuo Z, and Lin G (2007b) Intestinal and hepatic glucuronidation of flavonoids. *Mol Pharm* **4:**833–845.

Address correspondence to: Walter Brand, Division of Toxicology, Wageningen University, P.O. Box 8000, 6700 EA Wageningen, The Netherlands. E-mail: walter.brand@wur.nl